Acute Downregulation of ENaC by EGF Involves the PY Motif and Putative ERK Phosphorylation Site

Rebecca A. Falin[1] and Calvin U. Cotton[1,2]

[1]Department of Physiology and Biophysics and [2]Department of Pediatrics, Case Western Reserve University, Cleveland, OH 44106

The epithelial sodium channel (ENaC) is expressed in a variety of tissues, including the renal collecting duct, where it constitutes the rate-limiting step for sodium reabsorption. Liddle's syndrome is caused by gain-of-function mutations in the β and γ subunits of ENaC, resulting in enhanced Na reabsorption and hypertension. Epidermal growth factor (EGF) causes acute inhibition of Na absorption in collecting duct principal cells via an extracellular signal–regulated kinase (ERK)–dependent mechanism. In experiments with primary cultures of collecting duct cells derived from a mouse model of Liddle's disease (β-ENaC truncation), it was found that EGF inhibited short-circuit current (Isc) by 24 ± 5% in wild-type cells but only by 6 ± 3% in homozygous mutant cells. In order to elucidate the role of specific regions of the β-ENaC C terminus, Madin-Darby canine kidney (MDCK) cell lines that express β-ENaC with mutation of the PY motif (P616L), the ERK phosphorylation site (T613A), and C terminus truncation (R564stop) were created using the Phoenix retroviral system. All three mutants exhibited significant attenuation of the EGF-induced inhibition of sodium current. In MDCK cells with wild-type β-ENaC, EGF-induced inhibition of Isc (<30 min) was fully reversed by exposure to an ERK kinase inhibitor and occurred with no change in ENaC surface expression, indicative of an effect on channel open probability (P_o). At later times (>30 min), EGF-induced inhibition of Isc was not reversed by an ERK kinase inhibitor and was accompanied by a decrease in ENaC surface expression. Our results are consistent with an ERK-mediated decrease in ENaC open probability and enhanced retrieval of sodium channels from the apical membrane.

The Journal of General Physiology

INTRODUCTION

The epithelial sodium channel is found in the apical membrane of a number of epithelial tissues, including the renal tubule, airway epithelia, lining of the distal colon, and ducts of the exocrine glands. It is the rate-limiting step in the process of sodium reabsorption and is important for maintaining electrolyte and water balance and, thereby, blood pressure (Garty and Palmer, 1997). The channel consists of three subunits, α, β, and γ, each of which contains two membrane-spanning domains with intracellular N and C termini and a conserved cysteine-rich region in the extracellular loop. These characteristics are shared with *Caenorhabditis elegans* degenerins and other members of the DEG/ENaC superfamily (Lingueglia et al., 1993; Renard et al., 1994; Rotin et al., 1994; Snyder, 1994; Voilley et al., 1994, 1997). The stoichiometry of the active channel is generally thought to be 2α:1β:1γ, although other combinations have been proposed (Snyder et al., 1998; Rossier et al., 2002; Staruschenko et al., 2005). All three subunits also contain a conserved PY motif (PPXY) in their C terminus and lysines on their N terminus (Chen and Sudol, 1995). The α and γ subunits are proteolytically cleaved during maturation and/or after delivery to the plasma membrane, resulting in channel activation (Hughey et al., 2003; Sheng et al., 2006; Bruns et al., 2007).

The main physiological regulator of Na^+ reabsorption in the renal collecting duct is the steroid hormone aldosterone, which binds to mineralocorticoid receptor and is known to induce the transcription of a number of genes, including the α-subunit of ENaC, resulting in long-term increases in Na^+ transport (Schafer, 2002). Insulin and vasopressin also increase Na^+ transport in the collecting duct (Blazer-Yost et al., 1998; Morris and Schafer, 2002). The mechanisms responsible for increased sodium transport in epithelial cells are not fully understood, but increases in the number of active channels and/or channel open probability have been proposed (Rossier, 2002). The number of channels in the plasma membrane is determined by the rates of channel insertion and retrieval. The PY motifs, located in the intracellular C termini of the β- and γ-ENaC subunits, have been shown to play key role in removal of channels. The protein ubiquitin ligase Nedd4 contains tryptophan-rich WW domains, which bind to the PY motif on the β and γ subunits of ENaC (Staub et al., 1996). Nedd4 in turn polyubiquitinates ENaC on lysine residues on the N terminus and targets the channel for

Correspondence to Calvin U. Cotton: cuc@case.edu

Abbreviations used in this paper: BFA, brefeldin A; EGF, epidermal growth factor; ENaC, epithelial sodium channel; ERK, extracellular signal–regulated kinase; FACS, fluorescence-activated cell sorting; GM, growth media; IM, induction media; MAPK, mitogen-activated protein kinase; MDCK, Madin-Darby canine kidney.

internalization and degradation (Staub et al., 1997, 2000). The study of Liddle's syndrome has been instrumental in our understanding of this regulatory process. Liddle's syndrome is caused by one of a number of gain-of-function mutations in the β- or γ-subunit of ENaC that either abrogate most of the C terminus or disrupt the PY motif (Warnock, 2001; Hummler, 2003). Quantitative studies of channel function and surface expression suggested dual effects of Liddle's mutations on channel number and channel open probability (Firsov et al., 1996). The results of a recent study (Knight et al., 2006) suggest that Liddle's mutations increase ENaC expression in the plasma membrane as well as the fraction of cleaved, fully active channels.

Epidermal growth factor (EGF) is a potent activator of the extracellular signal–regulated kinases (ERK) in wide range of mammalian cells. ERK1 and ERK2, collectively referred to as ERK1/2, are members of the mitogen-activated protein kinase (MAPK) signaling cascade that translates external signals into intracellular responses (Cano and Mahadevan, 1995; Cobb, 1999; Pearson et al., 2001). EGF-induced activation of the ERK signaling cascade has been implicated in a variety of cellular functions, including cell migration, cell cycle progression, and differentiation (Kari et al., 2003). EGF modulates Na^+ transport in epithelial cells in a several ways. It stimulates transport through the Na^+-K^+-ATPase, but reduces the expression of ENaC mRNA in alveolar type II cells (Danto et al., 1998). In mouse renal collecting duct cells, EGF rapidly inhibits amiloride-sensitive sodium current in an ERK1/2-dependent manner and long-term exposure to EGF reduces ENaC mRNA expression (Shen and Cotton, 2003; Falin et al., 2005).

Protein phosphorylation/dephosphorylation is an important posttranslational modification implicated in a wide variety of regulatory functions. Increased phosphorylation of β- and γ-ENaC subunits in response to insulin was associated with an increase in channel function in A6 cells (Zhang et al., 2005). Three phosphorylation sites have been identified in the C-terminal tail of the β (and γ)-ENaC subunit. βS613 is phosphorylated by casein kinase 2 (Shi et al., 2002b), but the functional consequence of phosphorylation at this site has not been determined. The second site is at βS620 (γT630), and phosphorylation of this site has been linked with the serum glucocorticoid kinase (*sgk*)–related increase in channel activity (Chigaev et al., 2001). The third site is a putative ERK1/2 phosphorylation site located at βT613 (γT623), adjacent to the PY motif. Phosphorylation of this site has been shown to increase the association rate constant for the ENaC C terminus and the WW domain of the protein ubiquitin ligase Nedd4-2 (Shi et al., 2002a) and has been implicated in cAMP-dependent regulation of ENaC (Yang et al., 2006). The purpose of this study is to determine the role of the β-ENaC PY motif and putative ERK phosphorylation site in EGF-induced inhibition of sodium absorption in mammalian renal epithelial cells. We found that the acute inhibitory response to EGF was impaired by β-ENaC truncation and by point mutations in the PY motif and putative ERK phosphorylation site and that inhibition is due to sequential effects on channel activity and surface expression.

MATERIALS AND METHODS

Cell Culture

Madin-Darby canine kidney (MDCK) cells were maintained in growth media (GM), consisting of a 1:1 mixture of Dulbecco's modified Eagle's medium and Ham's F-12 medium and supplemented with 10% FBS, 2.5 mM L-glutamine, 50 U/ml penicillin, and 50 mg/ml streptomycin. ENaC expression was induced by growing of cells in induction media (IM) for 48 h. IM is serum-free GM that is supplemented with 1 μM dexamethasone and 2 mM sodium butyrate. The rationale for using serum-free media during the 48-h induction period is that inclusion of 10% serum caused nearly maximal ERK1/2 phosphorylation in these cells and limited our ability to acutely stimulate ERK1/2 phosphorylation with exogenous EGF. Cells were grown at 37°C with 5% CO_2 and passaged every 3–5 d.

Primary renal cells were obtained from freshly excised kidneys (Veizis et al., 2004; Falin et al., 2005). Kidneys were removed under sterile conditions from CO_2-anesthesized mice between the ages of 16 and 21 d. The renal capsule was peeled away and kidneys minced with a razor blade and rinsed in PBS. Samples were centrifuged at 20 *g* for 3 min and the PBS removed. The kidney tissue was then suspended in a solution of CT media containing 0.65 mg/ml Type IV collagenase and digested for 10–15 min in a 37°C water bath. Samples were again centrifuged and the media removed. Fresh CT media was added and digested tissue was resuspended and then plated onto plastic culture dishes. Media was changed every 48 h, for 6–8 d before sorting. In preparation for sorting, cells were detached from the plates with 0.25% trypsin in 0.5 mM EDTA, suspended in DMEM containing 10% FBS, and filtered through 40-μm mesh. Cells were centrifuged at 100 *g* for 5 min and the pellet resuspended in ice-cold PBS plus glucose, filtered again through 40-μm mesh cell strainers, and diluted to a density of ~20,000,000 cells/ml. Fluorescence-activated cell sorting (FACS) was conducted as described previously (Veizis and Cotton, 2005) using a Beckman Coulter Epics Elite cell sorter. CT media contains equal parts of DMEM and Ham's F-12 medium and is supplemented with 1.3 μg/liter sodium selenite, 1.3 μg/liter 3,3′5-triiodo-L-tyronine, 5 mg/liter insulin, 5 mg/liter transferrin, 25 mg/liter prostaglandin E1, 2.5 mM glutamine, and 50 nM dexamethasone.

Transepithelial Electrical Measurements

Cells were seeded onto collagen-coated permeable supports (Millicell CM filters, 12 mm; Millipore) at a density of 1.0 or 2.5×10^5 cells/filter for MDCK and primary renal cells, respectively, as described previously (Shen and Cotton, 2003; Veizis et al., 2004). MDCK cells were grown in IM for 2 d while primary renal cells were grown for 7–10 d at 37°C in CT media. Media was changed daily on filters. Filters were mounted in an Ussing chamber equipped with gas inlets and separate reservoirs for the perfusion of the apical and basolateral compartments with solutions maintained at 37°C with a circulating water jacket. Both sides were bathed in equal volumes of CT media that was oxygenated with 95% O_2, 5% CO_2 to maintain a pH of 7.4. Agar bridges were positioned 3 mm from the surface of the filters and the transepithelial voltage potential (V_T) measured. The current required to clamp the V_T to 0 mV (I_{SC}) was determined after compensation for solution and filter series resistance. The filters were maintained under

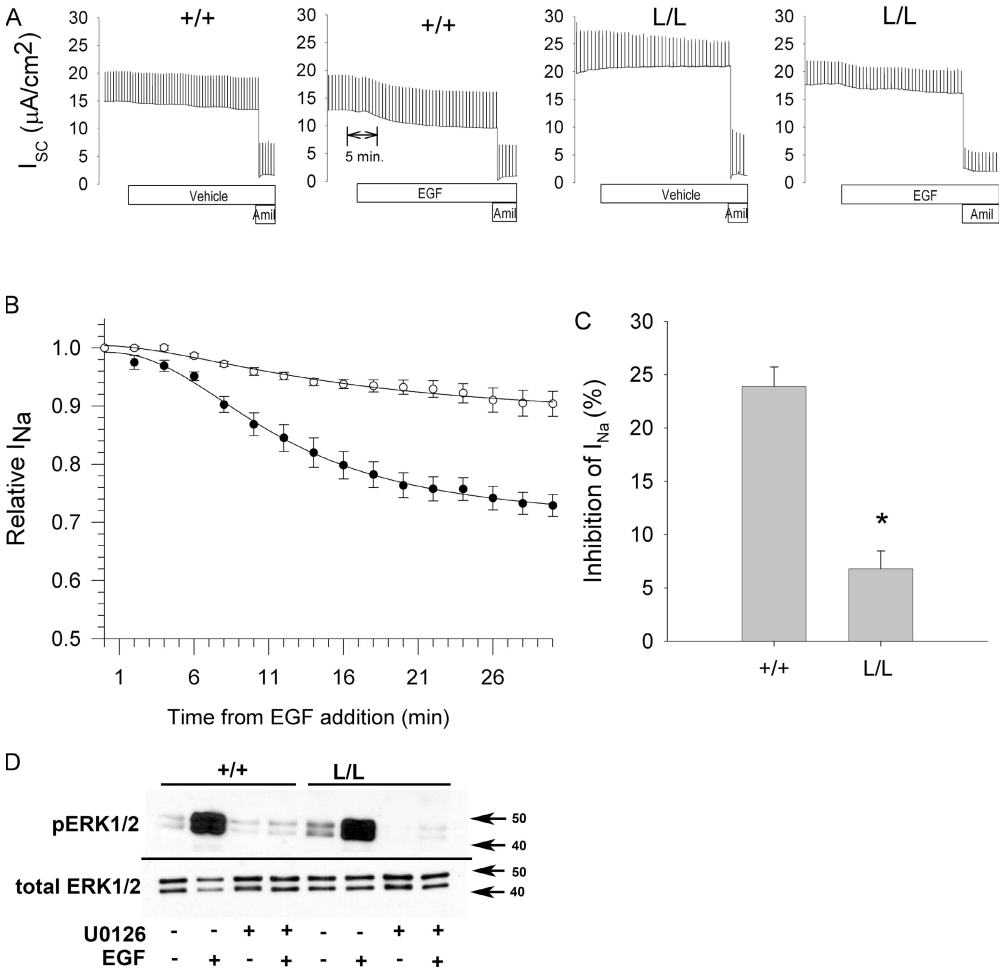

Figure 1. Effect of EGF on amiloride-sensitive I_{SC} and ERK1/2 phosphorylation in primary renal collecting duct cells. (A) Confluent monolayers of primary renal collecting duct cells isolated from homozygous wild type (+/+) or Liddle's (L/L) mice were mounted in Ussing chambers and bathed on both sides with CT media. At the indicated time either EGF (20 ng/ml) or vehicle was added to the basolateral compartment. After 30 min, amiloride (100 μM) was added to the apical compartment. The vertical deflections are at 1-min intervals and represent the change in current when the voltage is clamped to a nonzero value to measure transepithelial resistance. (B) Time course for EGF-induced inhibition of amiloride-sensitive I_{sc} (I_{Na}). Mean ± SEM for I_{Na} taken at 2-min intervals after addition of EGF (t = 0 min) to L/L (open circles; n = 8) or +/+ cells (closed circles; n = 9). (C) Summary of acute inhibition of I_{Na} 30 min after addition of EGF. n = 8–9. *, $P < 0.05$. (D) Western blot analysis of total and phosphorylated ERK1/2 in primary cultures of renal epithelial cells derived from either wild-type (+/+) or Liddle's (L/L) mice. Confluent monolayers were treated with EGF (20 ng/ml, basolateral) or vehicle for 30 min with and without a 15-min pretreatment with an ERK kinase inhibitor (U0126, 10 μM, apical/basolateral). Equivalent amounts of cell lysate (20 and 10 μg of cell lysate protein for total ERK1/2 and phosphorylated ERK1/2, respectively) were loaded into each lane. The blot is representative of three independent experiments.

short-circuit current conditions except for short intervals when the current is clamped to a nonzero value (1–5 mV) for 5 s to allow for the calculation of the transepithelial resistance (R_T).

Creation of MDCK Cell Lines

Mutagenesis was performed on rat βENaC within the PCR2.1 cloning vector using the QuikChange Site-directed Mutagenesis Kit (Stratagene) according to the manufacturer's instructions. Insertion of the FLAG tag into the extracellular loop between residues T137 and S138, a site that has been previously characterized as not affecting channel activity (Firsov et al., 1996), was accomplished with two rounds of mutagenesis using primers 5′-CCA CAG CAA CAC CAC CGA CTA CAA GGA CAG GAC CCT GAA CTT TAC CAT CTG G-3′ and 5′-CCA GAT GGT AAA GTT CAG GGT CCT GTC CTT GTA GTC GGT GGT GTT GCT GTG G-3′ for the first round and 5′-CCA CCG ACT ACA AGG ACG ACG ACG ACA AGA GGA CCC TGA ACT TTA CC-3′ and 5′- GGT AAA GTT CAG GGT CCT CTT GTC GTC GTC GTC CTT GTA GTC GGT GG-3′ for the second round. The G525C mutation was then made to the FLAG-tagged βENaC using primers 5′-CCT GGG GGG CCA GTT TTG CTT CTG GAT GGG GGG CTC GG-3′ and 5′-CCG AGC CCC CCA TCC AGA AGC AAA ACT GGC CCC CCA GG-3′. The single point mutations were then made in the G525C and FLAG-tagged βENaC with the primer sets 5′-GCA AAG GCC TGC GCA GGA GGT GAC CAC AGG CAC CC-3′ and 5′-GGG TGC CTG TGG TCA CCT CCT GCG CAG GCC TTT GC-3′; 5′-GCC CAT CCC GGG GAC TCC ACC CAA GAA CTA TGA CTC CCT GAG G-3′ and 5′-CCT CAG GGA GTC ATA GTT CTT GGG TGG AGT CCC CGG GAT GGG C-3′; 5′-GCC CAT CCC GGG GGC CCC ACC CCC-3′ and 5′-GGG GGT GGG GCC CCC GGG ATG GGC-3′; and 5′-CGT GTG GCT GCT CAA AAA CCT GGG GGG CC-3′ and 5′-GGC CCC CCA GGT TTT TGA GCA GCC ACA CG-3′ for R564stop, P616L, T613A, and S518K, respectively. All mutations were verified by sequencing.

A retroviral expression system was used in this study. βENaC was subcloned into the Phoenix retroviral vector, pBMN-I-GFP, a bicistronic vector that expresses GFP from an internal ribosomal entry site (IRES), allowing for positive selection by FACS. Directional subcloning was performed using the EcoRI and XhoI restriction sites. Proper orientation was verified by sequencing. The Phoenix amphotropic HEK293 packaging cell line was transfected with the retroviral plasmids using Fugene 6 (Roche) transfection reagent according to manufacturer's instructions. Subconfluent plates of MDCK cells were transduced with the resulting retroviral supernatant. For creation of clonal cell lines, MDCK cells were grown for 2 wk and then subjected to FACS. The sorted cells were returned to GM and grown for an additional 2 wk and subjected to FACS again. All cells exhibiting fluorescence readings greater than

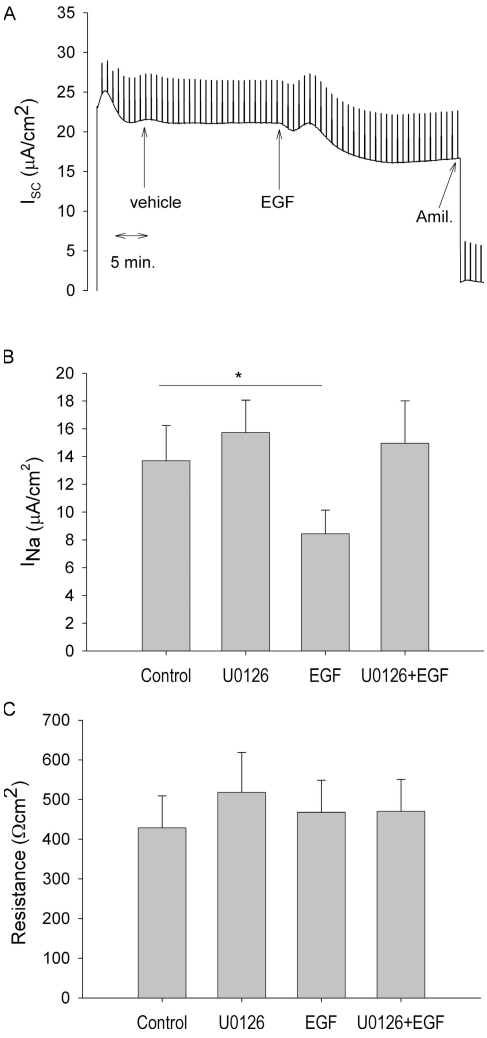

Figure 2. Effect of EGF on amiloride-sensitive I_{SC} in confluent monolayers of parental MDCK cells. Cells were seeded onto collagen-coated filters and grown in IM for 48 h. Filters were mounted in Ussing chambers and bathed on both sides with serum-free GM. (A) Representative trace. The epithelial monolayer was maintained under short-circuit conditions, and at 1-min intervals the voltage was clamped to a small nonzero value to measure transepithelial resistance. At the indicated time, EGF (20 ng/ml) was added to the basolateral compartment and 30 min later, amiloride (100 μM) was added to the apical compartment. (B and C) Summary of the effects of EGF and U0126 on I_{Na} and transepithelial resistance. Confluent monolayers of induced parental MDCK cells were mounted in Ussing chambers and after the current stabilized, vehicle (10 μl DMSO) or U0126 (10 μM, apical and basolateral) was added. 30 min later, vehicle or EGF (20 ng/ml, basolateral) was added followed 30 min later by amiloride (100 μM, apical). I_{Na} was calculated as the difference in I_{SC} immediately before and after addition of amiloride. Transepithelial resistance was measured near the beginning of the experiment after the current stabilized. $n = 5$ for each group. *, $P < 0.05$.

that exhibited by the parental cells were collected. At 5 wk the MDCK cells were subjected to single cell sorting into 96-well plates. Cells with fluorescence units at 10^3 or greater were designated high expression for use in this study. Cells with fluorescence in the range of 10^2–10^3 were designated medium expression and between 10^1 and 10^2 low expression. Control cells exhibited fluorescence between 10^0 and 10^1 units. Mixed populations of G525C and S518K were obtained by sorting cells that had been transduced 10 d earlier. Cells with fluorescence in the range of 10^2 and above were collected for study of mixed populations.

Western Blot and Immunoprecipitation

Cells were grown to confluence on 24-mm Transwell filters (Costar) and MDCK cells were maintained for 48 h in serum-free IM before cell harvest. Monolayers were washed with ice-cold PBS and then 120 μl of RIPA lysis buffer was added to the filter. RIPA lysis buffer consists of 50 mM Tris at pH 7.4, 0.10% IGEPAL, 2 mM EDTA, 1 mM EGTA, 150 mM NaCl, 0.10% SDS, 0.50% sodium deoxycholate, 50 μl/ml protease inhibitor cocktail in DMSO (Sigma-Aldrich), 5 μl/ml phosphatase inhibitor cocktail 2 (Sigma-Aldrich), 50 μM PMSF, 10 μM heat-activated sodium orthovanadate. Cells were then scraped off filters and the lysates transferred to 1.5-ml tubes. The lysates were passed several times through a 25-G needle attached to a 1-ml syringe and then precleared by centrifugation at 14,000 rpm for 10 min at 4°C in a microcentrifuge. The lysates were then transferred to a fresh 1.5-ml tube, being careful to not disturb the pellet of cellular debris in the bottom of the tube, and stored on ice. The total protein concentration in each sample was determined using a BCA kit (Pierce Chemical Co.) according to manufacturer's directions. Laemmli buffer containing β-mercaptoethanol was added to protein samples (10 μg for phospho-ERK and 5 μg for total ERK analysis), boiled for 4 min, and returned to ice for 1 min. Samples were run on 7.5% SDS-PAGE gels and transferred to nitrocellulose membranes. Membranes were probed with primary antibodies for p42/p44 (1:1,000, total ERK1/2; Cell Signaling Technologies) or phospho-p42/p44 (1:1,000, phospho-ERK1/2; Cell Signaling Technologies) and anti-rabbit HRP secondary antibody (1:1,000; Cell Signaling Technologies). Other blots were probed for the FLAG-tagged βENaC using anti-FLAG M2 coupled to HRP (1:1,000; Sigma-Aldrich). Blots were developed by ECL chemiluminescence.

For immunoprecipitation, cell lysates were prepared in nondenaturing lysis buffer (ND) consisting of 50 mM Tris at pH 7.4, 1% Triton X-100, 5 mM EDTA, 300 mM NaCl, 0.02% sodium azide, 50 μl/ml protease inhibitor cocktail in DMSO (Sigma-Aldrich), 5 μl/ml phosphatase inhibitor cocktail 2 (Sigma-Aldrich), 50 μM PMSF, and 10 μM heat-activated sodium orthovanadate. Lysates were precleared with protein G and proteins were immunoprecipitated with anti-FLAG M2 antibody (Sigma-Aldrich) and protein G beads (Sigma-Aldrich) overnight. Beads were then washed three times with IP wash buffer consisting of 50 mM Tris at pH 7.4, 0.10% Triton X-100, 5 mM EDTA, 300 mM NaCl, 0.02% sodium azide, 50 μl/ml protease inhibitor cocktail in DMSO (Sigma-Aldrich), 5 μl/ml phosphatase inhibitor cocktail 2 (Sigma-Aldrich), 50 μM PMSF, 10 μM heat-activated sodium orthovanadate. Proteins were eluted in laemmli buffer with 5% β-mercaptoethanol at 95°C for 5 min, separated by SDS-PAGE, and transferred to PVDF membranes (Millipore). Membranes were probed as described above for Western blots.

Surface Expression of βENaC

MDCK cells were grown to confluence on 24-mm Transwell filters (Costar). EGF (20 ng/ml) was added to the basolateral compartment for the indicated time. Filters were washed three times in ice-cold PBS and then biotinylated with sulfo-NHS-SS-biotin (Pierce Chemical Co.) according to a protocol modified from manufacturer's instructions. In brief, a solution of 1.0 mg/ml of sulfo-NHS-SS biotin in sodium borate buffer (85 mM NaCl, 4 mM KCl, 15 mM Na2B4O7, pH 8.5) was made immediately before use and applied to the apical compartment. The filters were then placed in a 4°C cold room on a rocker with gentle agitation for 30 min. Filters were then washed once with 25 mM Tris PBS to quench unreacted biotin and then three times with ice cold PBS.

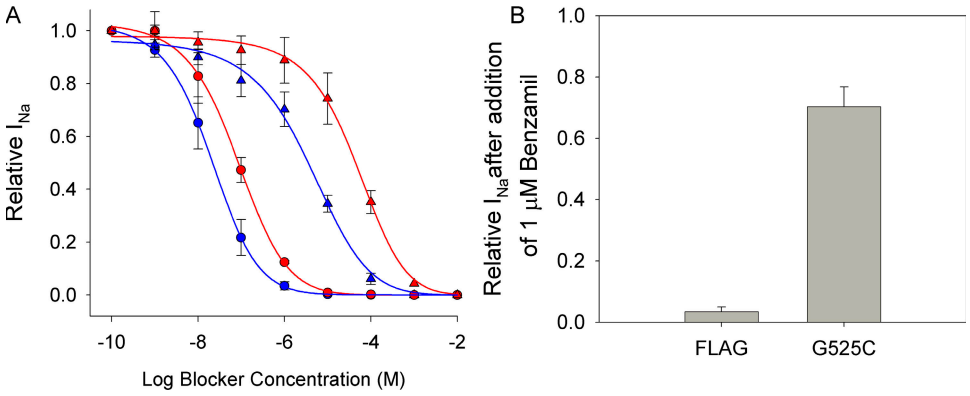

Figure 3. Dose–response relationships for amiloride and benzamil inhibition of I_{Na} in engineered MDCK cell lines transduced with the FLAG-tagged β-ENaC. Validation of the G525C mutation. (A) Monolayers of MDCK cells stably expressing FLAG-tagged β-ENaC (circles; FLAG) or FLAG-tagged/G525C β-ENaC (triangles; G525C) were grown to confluence and mounted in Ussing chambers. Increasing concentrations of benzamil (blue) and amiloride (red) were added to the apical compartment and the relative I_{Na} determined as the ratio of the I_{Na} at the indicated concentration and that at the start of the experiment. (B) The fraction of total I_{Na} that was insensitive 1 μM benzamil (i.e., channels with a G525C β-ENaC) in MDCK cell lines stably expressing FLAG-tagged β-ENaC (FLAG) or FLAG-tagged/G525C β-ENaC (G525C).

Cells were then lysed in ND buffer and total protein concentration determined by a bicinchoninic acid protein assay. Lysates containing 400 μg total protein were combined with streptavidin agarose beads and tumbled overnight at 4°C. The beads were pelleted by centrifugation and the supernatant was removed and labeled "cytosol." Sample buffer (2×) containing 5% β-mercaptoethanol was added to the beads, and beads were boiled for 3 min and then put on ice for 1 min. The entire volume was then applied to 5–20% gels, separated by SDS-PAGE, and transferred to PVDF membranes. At the same time the "cytosol" samples (20 μg total protein) were boiled with the proper volume of 5× sample buffer containing β-mercaptoethanol and applied to another 5–20% gel and treated in the same way. The surface (eluted from beads) and cytosol βENaC was detected by an anti-FLAG M2 antibody and visualized by chemiluminescence. The blots were stripped and probed with anti-actin to confirm that cytosolic proteins were not labeled with biotin.

Transgenic Mice

The Liddle's syndrome mice, generated by insertion of a stop codon corresponding to the human R566 residue into the βENaC gene, were described previously (Pradervand et al., 1999). The Liddle's mice were bred with the Hoxb7/EGFP transgenic line, which expresses enhanced green fluorescent protein specifically in the collecting ducts. Pups were genotyped for the R566X-truncation and the GFP transgene ($GFP^{+/?}$) as previously described (Pradervand et al., 1999; Srinivas et al., 1999). F2 pups that were either homozygous mutant (L/L) or wild-type (+/+) for β-ENaC and carried the GFP transgene were selected for isolation, sorting, and culture of collecting duct cells.

Statistical Analysis

All results are expressed as mean ± SEM. Statistical significance was evaluated by either paired or unpaired Student's *t* test. $P < 0.05$ was considered significant.

RESULTS

Deletion of the β-ENaC Subunit C Terminus Blocks EGF-induced Inhibition of Amiloride-sensitive Sodium Absorption

Previous studies have demonstrated EGF-induced inhibition of ENaC-mediated sodium absorption in murine renal collecting duct cells. The inhibitory response developed rapidly (5–20 min) and required activation of the ERK1/2 MAP kinase signaling cascade; however, the mechanism for this acute reduction in ENaC activity was not explored. A putative ERK1/2 phosphorylation site is located in the C terminus of β-ENaC (β−T613) and phosphorylation of the site is proposed to increase binding of a ubiquitin ligase Nedd4, channel ubiquintylation, and internalization. A mouse model of Liddle's syndrome in which the C terminus of β-ENaC is truncated (R564stop), was used to determine if an intact β-ENaC is required for EGF-induced inhibition of sodium absorption. Amiloride-sensitive short-circuit current was measured in primary cultures of renal collecting duct epithelial cells derived from wild type (+/+) and homozygous mutant (L/L) mice. As expected, the cells isolated from mice homozygous for the Liddle's mutation (L/L) exhibited a higher amiloride-sensitive I_{SC} (16.3 ± 1.5 μA/cm^2; $n = 8$) than their wild-type (+/+) littermates (12.3 ± 2.1 μA/cm^2; $n = 9$). In both cases, >90% of the I_{SC} was inhibited by amiloride. Addition of EGF to the basolateral bathing solution elicited the characteristic decline in I_{SC} in monolayers of wild-type cells (+/+); however, the response of monolayers of mutant cells (L/L) was substantially reduced (Fig. 1 A). Summary data for the time course of EGF-induced inhibition of amiloride-sensitive short-circuit current (I_{Na}) in +/+ and L/L monolayers is shown in Fig. 1 B. The EGF-induced decrease in amiloride-sensitive I_{SC} for monolayers of L/L cells is significantly attenuated compared with that of the +/+ cells (∼75%; Fig. 1 C). The EGF-induced increase in ERK1/2 phosphorylation is similar in collecting duct cell monolayers from +/+ and L/L mice (Fig. 1 D). Deletion of the intracellular β-ENaC C terminus eliminates several consensus phosphorylation sites as well as two internalization motifs (PY and YXXφ). To explore the importance of the PY motif and putative ERK phosphorylation site in the acute downregulation of ENaC by EGF-induced ERK1/2 activation, a stable mammalian expression system was developed.

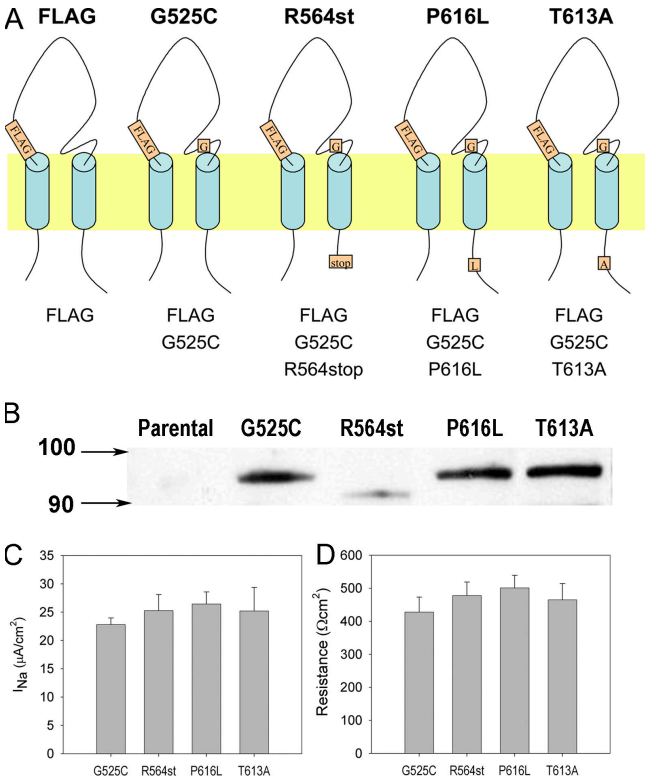

Figure 4. Creation of the MDCK cell lines stably expressing engineered β-ENaC. (A) Diagrammatic representation of the modifications/mutations introduced into β-ENaC and stably expressed in MDCK cells. The name of each cell line is listed above and the modifications/mutations present within the channel are below the drawing. (B) Parental and clonal cell lines were harvested and analyzed for expression of the FLAG-tagged β-ENaC subunit. Anti-FLAG M2 antibody was used to immunoprecipitate FLAG-tagged β-ENaC from cell lysates. Bound proteins were eluted, separated by SDS-PAGE, and probed with an M2 anti-FLAG antibody. (C) Summary of I_{Na} in confluent monolayers of clonal MDCK cell lines stably expressing modified/mutated βENaC subunits ($n = 5$). I_{Na} was calculated as the fraction of I_{SC} that was insensitive to 1 μM benzamil, but blocked by 10 mM amiloride. (D) Summary of transepithelial resistance in MDCK cell lines ($n = 5$).

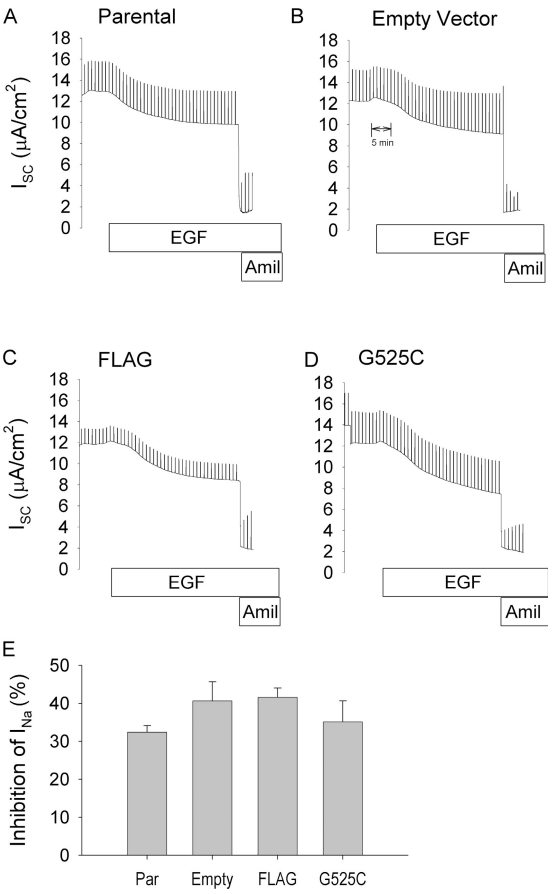

Figure 5. Effect of EGF on short-circuit current in parental and modified MDCK cell lines. Parental MDCK cells were transduced with empty retroviral vector, FLAG-tagged wild-type β-ENaC, or FLAG-tagged/G525C β-ENaC (all transduced lines express GFP under the control of IRES). (A–D) Cells were grown to confluence on filters and mounted in Ussing chambers. After currents stabilized, EGF (20 ng/ml, basolateral) was added followed 30 min later by amiloride (10 mM, apical for G525C; 100 μM, apical for others). (E) Summary of EGF-induced inhibition of I_{Na} ($n = 5$ for each cell line).

Generation and Characterization of MDCK Cell Lines with Stable Expression of Mutant β-ENaC

Type I MDCK cells form high-resistance polarized epithelial monolayers. A MDCK line with inducible expression of all three subunits of rat ENaC from a tricistronic vector was chosen as the parental cell line for these studies (Stutts et al., 1995). To confirm that EGF-induced inhibition of sodium transport was retained in this cell line, ENaC expression was induced in confluent monolayers of parental MDCK cells for 48 h and the effect of EGF on amiloride-sensitive short-circuit current was accessed. A representative trace shows that MDCK monolayers generate a large I_{sc} and addition of EGF to the basolateral bathing solution reduces I_{sc} by ~30% (Fig. 2 A). Subsequent addition of amiloride to the apical bathing solution reduces the I_{sc} to near zero. If the monolayer is first treated with amiloride, I_{sc} is reduced to near zero, and subsequent exposure to EGF does not further reduce I_{sc} (unpublished data). Additional experiments were done to confirm that the EGF-induced inhibition of sodium absorption required ERK1/2 phosphorylation. Pretreatment of MDCK monolayers with an ERK kinase inhibitor (U0126) prevents ERK1/2 phosphorylation and EGF-induced inhibition of amiloride-sensitive I_{sc} as was observed in previous studies of mouse renal collecting duct cell monolayers (Veizis et al., 2004; Falin et al., 2005; Veizis and Cotton, 2005). The effects of EGF and U0126 on I_{Na} and transepithelial resistance are summarized in Fig. 2 (B and C).

A retroviral expression system was used to introduce engineered forms of β-ENaC into parental MDCK cells. Since the parental MDCK cell line expresses wild-type β-subunit, it was necessary to use β-ENaC constructs that contain an inserted extracellular FLAG epitope and a G525C mutation. The G525C mutation shifts the K_i for

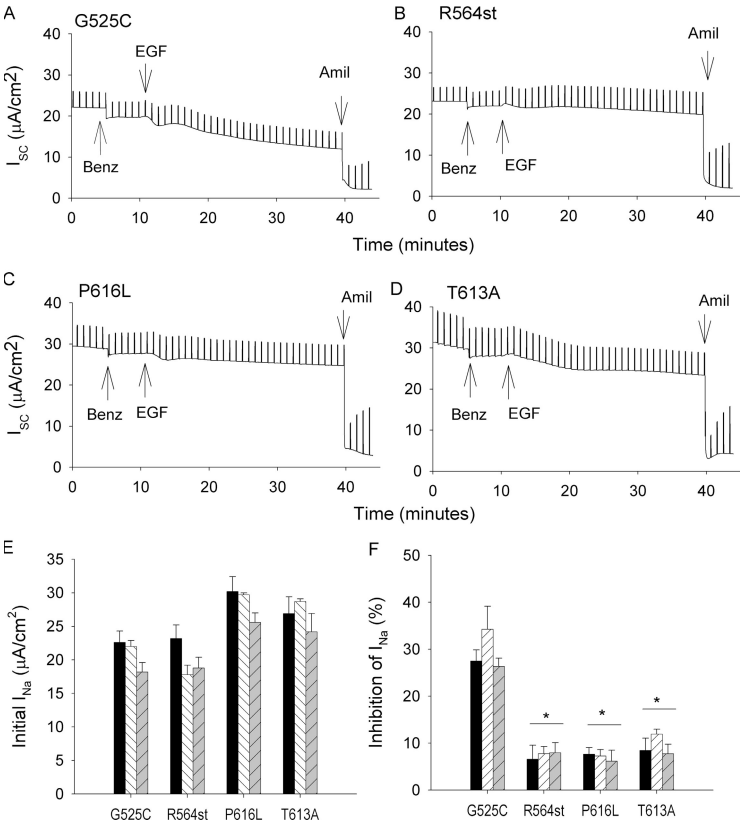

Figure 6. Effect of EGF on short-circuit current in MDCK cell lines stably expressing mutant β-ENaC subunits. (A–D) Representative traces of short-circuit current in confluent monolayers of G525C, R564st, P616L, and T613A MDCK cell lines. At the indicated times benzamil (1 μM, apical), EGF (20 ng./ml, basolateral), and amiloride (10 mM, apical) were added. (E) The initial I_{Na} is the benzamil-insensitive, amiloride-sensitive, short-circuit current measured in three independent clonal cell lines for each mutation (n = 5 filters for each clone). (F) Summary of EGF-induced inhibition of I_{Na} in three independent clonal cell lines for each mutation (n = 5 filters for each clone). *, $P < 0.05$.

amiloride and benzamil block to higher concentrations and allows a functional distinction between channels that contain a wild-type verses a modified β-subunit (Schild et al., 1997). Parental MDCK cells were transduced with β-subunit containing both the FLAG tag and the G525C mutation or the FLAG tag alone. The benzamil and amiloride dose–response curves for inhibition of I_{sc} in cells that express FLAG-tagged β-ENaC subunits yield K_is of 18 and 84 nM; whereas the K_is for benzamil and amiloride were shifted to 2.9 and 36 μM in cells that express the G525C mutation (Fig. 3 A). Application of 1 μM benzamil blocks essentially all of the amiloride-sensitive I_{sc} due to ENaC channels that contain a β-ENaC subunit that lacks the G525C mutation (i.e., endogenous wild-type channels), while leaving most of the current through channels containing the β-ENaC G525C mutation (Fig. 3). Channels that contain a β-ENaC subunit with the G525C mutation are blocked by 10 mM amiloride. Thus, the modifications to β-ENaC confer unique functional and biochemical attributes to channels that contain the engineered subunit.

Three types of mutations were introduced into the β-ENaC subunit in order to evaluate the importance of specific sites in ERK-dependent inhibition of sodium transport. A truncation mutation (R564st) to mimic the Liddle's mouse model, a PY motif mutation (P616L), and a mutation in the putative ERK phosphorylation site located adjacent to the PY motif (T613A). MDCK cells were transduced with the β-ENaC subunit containing the FLAG tag, the G525C mutation, and one of the three additional mutations (Fig. 4 A). Stable MDCK cell lines were created by FACS-positive selection, and expression of the mutant β-ENaC subunit was confirmed (Fig. 4 B). MDCK cells from each of the cell lines were seeded onto permeable supports, grown to confluence, and wild-type ENaC expression was induced for 48 h before electrophysiological characterization. The amiloride-sensitive I_{sc} and transepithelial resistance for each cell line are summarized in Fig. 4 (C and D). The values for amiloride-sensitive I_{SC} and transepithelial resistance were not significantly different among the cell lines that carried the mutant β-ENaC subunit or compared with the parental line (Fig. 4, C and D).

EGF-induced Inhibition of Sodium Transport Requires ERK1/2 Phosphorylation and an Intact β-ENaC Subunit

The effect of EGF on sodium absorption was evaluated in confluent monolayers maintained under short-circuit conditions in Ussing chambers. In the case of the G525C mutation cell line, it was necessary to add 1 μM benzamil to the apical bathing solution to block endogenous channels that contain wild type β-ENaC subunit. Representative traces are illustrated in Fig. 5 (A–D) and the summary data in Fig. 5 E. In each cell line tested, EGF treatment elicited the characteristic 30–40% reduction in amiloride-sensitive I_{sc}.

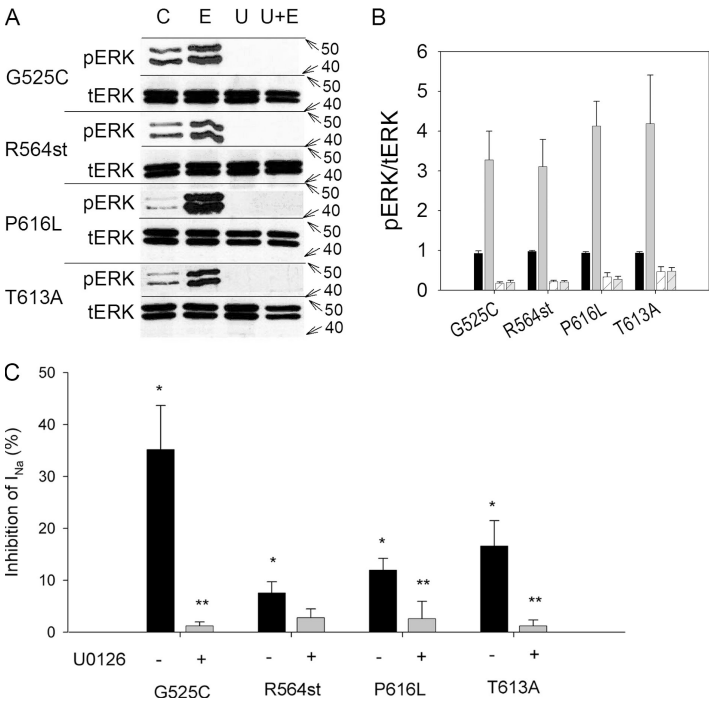

Figure 7. EGF-induced ERK1/2 phosphorylation and p-ERK1/2–dependent inhibition of I_{Na} in MDCK cell lines. G525C, R564st, P616, and T613A MDCK cell lines were grown to confluence on filters and bathed in IM for 48 h. (A) Individual monolayers were treated with vehicle (lane C; DMSO, 10 μl, both sides, 45 min), EGF (lane E; EGF, 20 ng/ml, basolateral, 15 min), ERK kinase inhibitor (U; U0126, 10 μM, both side, 45 min), or ERK kinase inhibitor plus EGF (U + E; U0126, 10 μM, both side, 30 then EGF, 20 ng/ml, basolateral, 15 min). Cells were then lysed, separated by SDS-PAGE, and probed for phosphorylated ERK1/2 and total ERK1/2. The blots are representative of three independent experiments. Densitometry was performed on each blot and the ratio of pERK1/2 to total ERK1/2 was determined for each cell line under each condition and the data are summarized in B. (C) Confluent monolayers of G525C, R564st, P616L, and T613A MDCK cell lines were exposed to EGF (20 ng/ml, 30 min, basolateral) with or without pretreatment with an ERK kinase inhibitor (U0126; 10 μM, 15 min, bilateral). The inhibition of I_{Na} was calculated as previously described. $n = 5$. $P < 0.05$. *, significantly different compared with G525C control; **, significantly different compared with monolayers not treated with U0126.

The effect of EGF on ENaC-mediated sodium absorption in MDCK cell lines that express mutant β-ENaC was determined. Endogenous channels that contain wild-type β-ENaC were blocked by addition of 1 μM benzamil to the apical bathing solution followed by addition of EGF (20 ng/ml) to the basolateral bathing solution. Representative traces from each of the four cell lines are shown in Fig. 6 (A–D). In each case, benzamil reduced I_{sc} by ~10%, indicating that only a small fraction of the current was due to channels that contained a wild-type β-ENaC subunit with the majority of the current carried by channels that contained a mutant β-ENaC subunit. EGF treatment resulted in ~30% reduction in I_{sc} in the G525C cell line with only small inhibitory responses in the R564st, P616L, and T613A cell lines. Since the site of retroviral integration into the MDCK cell genome is undefined, it was necessary to evaluate multiple clonal cell lines to ensure that location of integration of the vector was not the cause of differences observed in the cell lines. Three clonal cell lines for each mutation were generated and evaluated and the results are summarized in Fig. 6 (E and F). The amiloride-sensitive short circuit currents and the effects of EGF on I_{sc} were similar within the clonal lines for each mutation. Amiloride-sensitive I_{SC} was the same for the G525C and the R564st mutation, while it was slightly increased in P616L and T613A mutations (Fig. 6 E). Monolayers of G525C clonal cell lines exhibited 28–35% acute inhibition in response to EGF while the R564st and P616L clonal cell lines were inhibited by 6–9% and the T613A clonal cell lines 8–12% (Fig. 6 F).

Previous studies have shown that EGF-induced inhibition of sodium transport in renal epithelial cells is ERK1/2 dependent. EGF-induced ERK1/2 phosphorylation was evaluated in confluent monolayers of G525C, R564st, P616L, and T613A cell lines. Addition of EGF to the basolateral bathing solution for 15 min increased ERK1/2 phosphorylation (pERK1/2) three to fourfold with no effect on total ERK1/2 (tERK1/2) (Fig. 7, A and B). Exposure to an ERK kinase inhibitor (U0126) reduced basal pERK1/2 and completely blocked EGF-induced ERK1/2 phosphorylation. In a parallel series of experiments, the effect of the ERK kinase inhibitor on EGF-induced inhibition of I_{sc} was evaluated. As shown in Fig. 7 C, pretreatment with U0126 completely prevented the 35% decrease in I_{sc} in G525C monolayers in response to EGF. Interestingly, the small inhibitory response to EGF observed in P616L and T613A β-ENaC cell lines was also blocked by U0126. Together these results suggest that both the PY motif and the putative ERK phosphorylation site in the β-ENaC subunit of the channel are required for full ERK1/2-mediated acute inhibition of ENaC activity and sodium absorption.

EGF-induced Inhibition of Sodium Absorption Is due to Sequential Effects on Channel Activity and Surface Expression

Liddle's syndrome mutations have been associated with reduced channel endocytosis and enhanced surface expression presumably due to elimination or disruption of the PY motif in the C terminus of β- and γ-ENaC subunits. Acute inhibition of sodium absorption is consistent with an ERK1/2-mediated decrease in ENaC

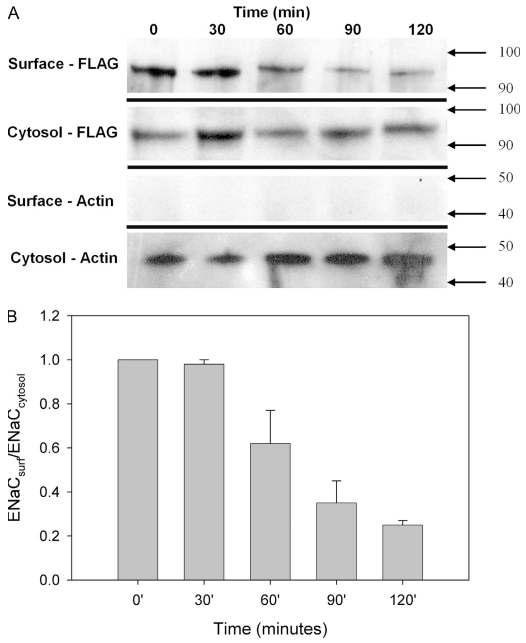

Figure 8. Time course for EGF-induced decrease in β-ENaC surface expression. (A) Surface expression of β-ENaC was determined by biotinylation and recovery of labeled apical membrane proteins by incubation with streptavidin beads. Biotinylated apical membrane and cytosolic protein samples were loaded on gels, separated by SDS-PAGE, transferred to nitrocellulose membranes, and probed with the M2 anti-FLAG antibody coupled to HRP to detect β-ENaC. The membranes were stripped and probed for actin. (B) Densitometry was performed and the ratio of surface to cytosol β-ENaC was determined for each sample and normalized to the ratio obtained at $t = 0$. $n = 4$. *, significantly different compared with ratio at $t = 0$. $P < 0.05$.

surface expression since EGF-induced inhibition is almost completely prevented by the R564st and P616L mutations. However, the inhibitory response could be due to a decrease in channel open probability and/or a reduction in the number of active channels at the apical surface (decreased delivery/increased retrieval). The surface expression of ENaC was evaluated by biotinylation of apical membrane proteins followed by immunoprecipitation and immunoblot. Confluent monolayers of G525C MDCK cells were treated with EGF for 0, 30, 60, 90, and 120 min and then analyzed for total and surface expression of ENaC. A representative immunoblot of surface and cytosolic ENaC is shown in Fig. 8 A and the results of all experiments are summarized in Fig. 8 B. Surface expression of ENaC was not decreased 30 min after EGF treatment, a time when the acute inhibitory response is fully developed. However, there was a significant reduction in surface expression of ENaC at later time points (60, 90, and 120 min). The temporal dissociation between EGF-induced inhibition of I_{sc} (<30 min) and decline in surface expression (>30 min) suggests that the initial response may be a decrease in channel open probability rather than retrieval from the apical membrane. To investigate this possibility, the βS518K mutation, which when expressed in oocytes increases the open probability of ENaC from ~0.5 to nearly twice that, was used (Condliffe et al., 2004). In our study the I_{Na} exhibited by the S518K mutant was not higher than G525C MDCK cells, as shown in Fig. 9 A. However, the percent inhibition by EGF exhibited by the S518K mutant was significantly greater than in G525 cells (Fig. 9 B).

A potential complication of this analysis is that under certain conditions large numbers of ENaC channels are present at the plasma membrane in an inactive or silent state, presumably because they were not proteolytically cleaved and activated during channel assembly and maturation. In this case biochemical assays of channel number and functional assays of channel activity may not correlate. Silent or low activity channels can be activated by brief exposure to extracellular trypsin. To determine if there was a significant population of silent, uncleaved channels that could distort the biochemical analysis of surface expression, the effect of trypsin on amiloride-sensitive I_{sc} was evaluated in MDCK cell monolayers. Immediately after addition of trypsin (3 μg/ml) to the apical surface of confluent MDCK cell monolayers there is a transient spike in I_{sc} followed by a small increase in I_{sc} compared with the initial value (Fig. 10 A). The transient increase in I_{sc} is not due to activation of silent ENaC channels since addition of amiloride (100 μM, apical) to block ENaC before trypsin did not alter the transient current, but did prevent the small steady-state increase in I_{sc} (Fig. 10 B). The small increase in current was also observed in MDCK monolayers treated with EGF before exposure to trypsin (Fig. 10 C). There also was no difference in the small trypsin-induced increase in current between G525C, P616L, and T613A MDCK cell monolayers (Fig. 10 D). The data suggest that under these experimental conditions, relatively few silent, trypsin-activatable sodium channels are present in the apical plasma membrane, and biochemical estimates of surface expression are valid.

Since there is no change in surface expression of ENaC for at least 30 min after exposure to EGF, it is possible that ERK1/2-dependent inhibition of I_{sc} is due to a reduction in channel open probability and should be reversible. Previous studies in collecting duct cell lines demonstrated that EGF-induced ERK1/2 phosphorylation and inhibition of amiloride-sensitive I_{sc} were readily reversed by treatment with an ERK kinase inhibitor (U0126) (Falin et al., 2005). To determine if there is a window of time during which the inhibitory response is reversible, the ERK kinase inhibitor was added 15, 30, 45, or 60 min after EGF treatment of MDCK cell monolayers. Summary traces are shown in Fig. 11 (A–D). The EGF-induced inhibition of I_{sc} is completely reversible at 15 and 30 min, partially reversible at 45 min, and almost completely irreversible at 60 min (Fig. 11, E and F).

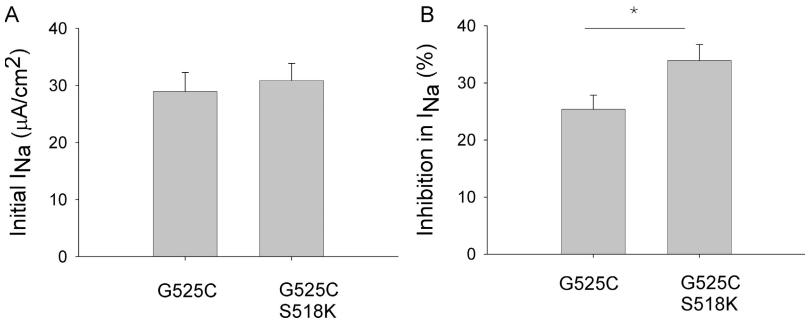

Figure 9. EGF-induced inhibition of I_{Na} in βG525C and βG525C/S518K mutant cell lines. Cells were grown to confluence on filters and mounted in Ussing chambers. After currents stabilized, benzamil (1 μM, apical) was added followed 5 min later by EGF (20 ng/ml, basolateral) addition, followed 30 min later by amiloride (10 mM, apical). (A) Initial I_{Na} was calculated as the I_{SC} immediately before addition of EGF minus the I_{sc} after addition of amiloride. (B) Summary of EGF-induced inhibition of I_{Na} ($n = 6$ for each cell line). *, $P < 0.05$.

ERK1/2-dependent Inhibition of Sodium Transport Is Not due to a Reduction in Channel Delivery

Under steady-state conditions where I_{sc} is constant, the rates of delivery and retrieval of ENaC from the apical plasma membrane should be equivalent. In principle, EGF-induced inhibition of I_{sc} could result from a reduction in the rate of channel delivery to the membrane. Brefeldin A (BFA), which blocks transport of protein from the ER to the Golgi network, was used to inhibit the trafficking of new ENaC channels to the plasma membrane. As illustrated in Fig. 12 (A and B) and summarized in Table I, in the presence of BFA, the rates of decline of amiloride-sensitive I_{sc} were not significantly different in G525C and T613A MDCK monolayers. Furthermore, the functional half-life following BFA treatment is similar to the half-life for surface expression of ENaC recently reported in another MDCK cell line expressing wild-type and Liddle's mutant ENaC (Chen et al., 2007). However, in monolayers treated with U0126 to reduce ERK1/2 phosphorylation, the rate of decline in I_{sc} was significantly reduced in G525C monolayers but was unaffected in T613A monolayers. Furthermore, in monolayers treated with EGF, the rate of decline in I_{sc} in G525C cells was significantly greater than T613A cells. Thus, the p-ERK1/2–dependent decrease in I_{sc} was approximately two times greater in G525C monolayers compared with monolayers of cells that carried a mutation in the putative ERK1/2 phosphorylation site (T613A) in the C terminus of β-ENaC (Table I).

DISCUSSION

We demonstrated previously that activation of the RAF/MEK/ERK signaling cascade by exposure to EGF results in biphasic inhibition of amiloride-sensitive sodium absorption in renal collecting duct cells. Prolonged activation causes a 50–60% reduction in sodium current and a 70–85% decrease in expression of ENaC subunit mRNAs (Shen and Cotton, 2003); whereas the early inhibitory phase develops within minutes and cannot be attributed to changes in ENaC expression (Falin et al., 2005). The acute, EGF-induced inhibition of epithelial sodium channel activity is thought to involve changes in channel gating and/or channel retrieval from the plasma membrane. The results of the present study demonstrate that there are critical sites in the intracellular C

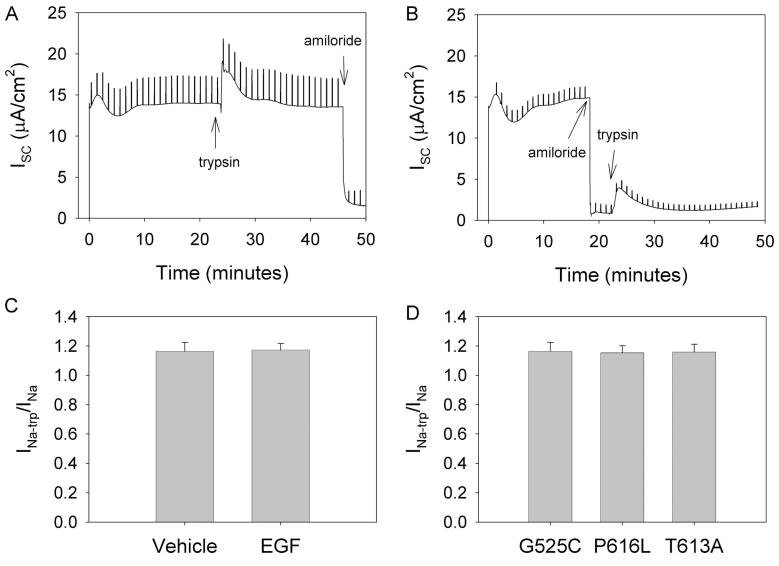

Figure 10. Effect of EGF and β-ENaC mutations on activation of amiloride-sensitive short-circuit current by trypsin. (A) Representative trace of a parental MDCK cell line monolayer mounted in an Ussing chamber and exposed to apical trypsin (3 μg/ml) followed by amiloride (10 μM). (B) Representative trace of a parental MDCK cell line monolayer treated with apical amiloride (10 μM) followed by trypsin (3 μg/ml). (C) Confluent monolayers of G525C MDCK cells were mounted in Ussing chambers and treated with benzamil (1 μM, apical) to block endogenous sodium channels. 5 min later, either vehicle or EGF (20 ng/ml, basolateral) was added. At 35 min, trypsin (3 μg/ml, apical) was added, and at 50 min amiloride (10 mM, apical) was added. $I_{Na\text{-}trp}/I_{Na}$ was calculated from the I_{Na} 15 min after trypsin addition divided by the I_{Na} immediately before trypsin addition. (D) G525C, P616L, and T613A MDCK cell line monolayers were mounted in Ussing chambers. Benzamil (1 μM, apical) was added at the start of the experiment, at 5 min trypsin (3 μg/ml, apical) was added followed by amiloride (10 mM, apical) at 20 min. The $I_{Na\text{-}trp}/I_{Na}$ was calculated as above.

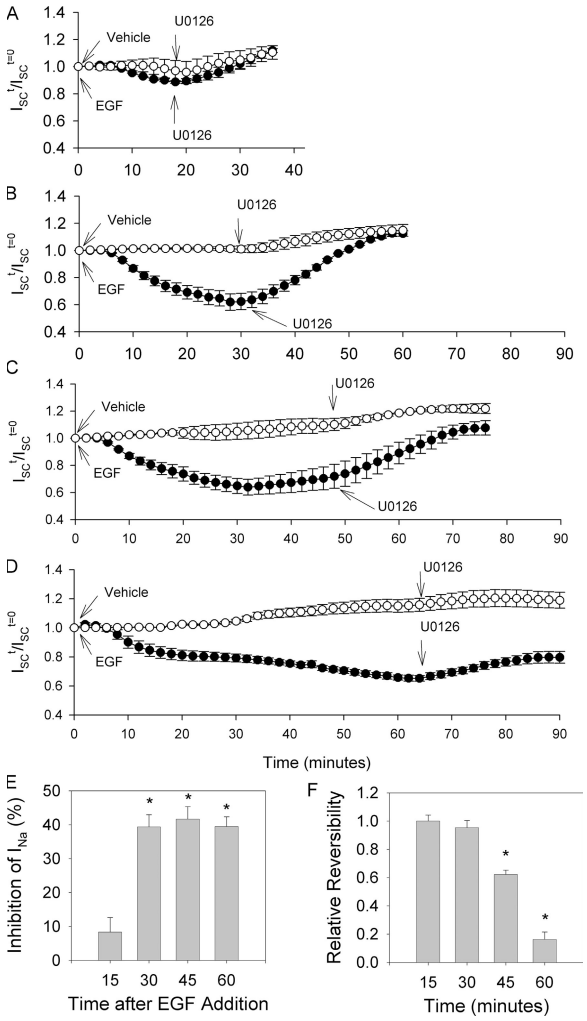

Figure 11. Reversibility of EGF-induced inhibition of amiloride-sensitive short-circuit current by an ERK kinase inhibitor. (A–D) Confluent monolayers of G525C MDCK cells were mounted in Ussing chambers and benzamil (1 μM) was added to the apical compartment. After the currents stabilized, EGF or vehicle (media) was added to the basolateral compartment. At various times thereafter (15, 30, 45, and 60 min), U0126 (10 μM) was added to the apical and basolateral compartments. Amiloride (10 mM) was added to the apical compartment at the end of experiment. The $I_{SC}^{t}/I_{SC}^{t=0}$ was calculated as the ratio of the I_{SC} at each time point divided by the I_{SC} at $t = 0$. Values represent mean ± SEM of the I_{sc} recorded at 2-min intervals. (E) Summary of the time course for EGF-induced inhibition of amiloride-sensitive short-circuit current. EGF-induced inhibition in I_{Na} was calculated immediately before the addition of U0126 as difference between the $I_{SC}^{t}/I_{SC}^{t=0}$ for cells treated with EGF and those treated with vehicle. $n = 5$, $P < 0.05$. *, significantly different from zero. (F) The relative reversibility of EGF-induced inhibition of I_{sc} was determined 30 min after the addition of U0126. It was calculated as the $I_{SC}^{t=end}/I_{SC}^{t=0}$ for EGF-treated cells divided by the $I_{SC}^{t=end}/I_{SC}^{t=0}$ for vehicle-treated cells. $n = 5$, $P < 0.05$. *, significantly different from 1.

terminus of β-ENaC that are required for ERK1/2-dependent inhibition of sodium current and that the inhibitory response is due to sequential effects on channel activity and surface expression.

TABLE I

Rates of Change in $I_{SC,amil}$ in BFA-treated Monolayers

	G525C	T613A
	%/min	*%/min*
Vehicle	−1.06 ± 0.22	−0.78 ± 0.10
EGF	−3.73 ± 0.25	−2.61 ± 0.26[a]
U0126	+0.12 ± 0.46	−0.80 ± 0.04[a]
U0126-EGF	3.85 ± 0.52	1.81 ± 0.26[a]

The rate of decline in I_{SC} in BFA-treated monolayers was determined. The monolayers were treated as described in Fig. 12. The ERK-dependent decline in I_{SC} was calculated as the difference between the rates for EGF and U0126 treated monolayers. $n = 5$ for each group.
[a]Significant difference between response in G525C cells, $P < 0.05$.

Truncation of β-ENaC C Terminus

Pradervand et al. (1999) generated a mouse model for Liddle's syndrome by insertion of a stop codon in the mouse β-ENaC gene locus (R564st). The heterozygous and homozygous mutant mice failed to exhibit the Liddle's phenotype (i.e., hypokalemia, metabolic alkalosis, and hypertension) until placed on a high salt diet, most likely due to poor expression of the mutant β-ENaC subunit. In vivo manipulations such as aldosterone infusion, dietary sodium restriction, and a high- K diet were found to cause exaggerated increases in amiloride-sensitive sodium current in cortical collecting duct cells from Liddle's mice, primarily attributable to an increase in channel density (Dahlmann et al., 2003). In vitro studies of murine collecting duct cell lines transfected with the R564st mutation demonstrated that induction of sodium absorption by aldosterone was similar between wild-type and mutant channels; however, downregulation of sodium current following aldosterone withdrawal was significantly slowed in cells with mutant ENaC (Auberson et al., 2003). Interestingly, transition from low-sodium to high-sodium diet elicited a rapid redistribution of ENaC from the apical membrane to the cytoplasm in connecting tubules from wild-type mice but not Liddle's mice (Pradervand et al., 2003). EGF-induced inhibition of amiloride-sensitive I_{sc} in primary culture collecting duct cells isolated from Liddle's mice and MDCK cells that express the R564st β-ENaC mutation was substantially reduced (Figs. 1 and 6). Although the acute inhibition of I_{sc} by EGF was greatly reduced, it was not completely abolished. This finding suggests that the C terminus of the γ-subunit is sufficient for partial EGF-induced inhibition, while the C termini of both the β and γ subunits are required for the full inhibitory effect to occur. Michlig et al. (2005) reported that truncation of all three ENaC subunits prevented progesterone-induced inhibition of sodium current in an oocyte expression system. It is also possible however that there are parallel actions of EGF on ENaC activity, one that depends on the intact C terminus of the β-subunit and another that does not. For example, heterologous expression of ENaC and the EGF receptor in CHO cells reconstituted a response in which

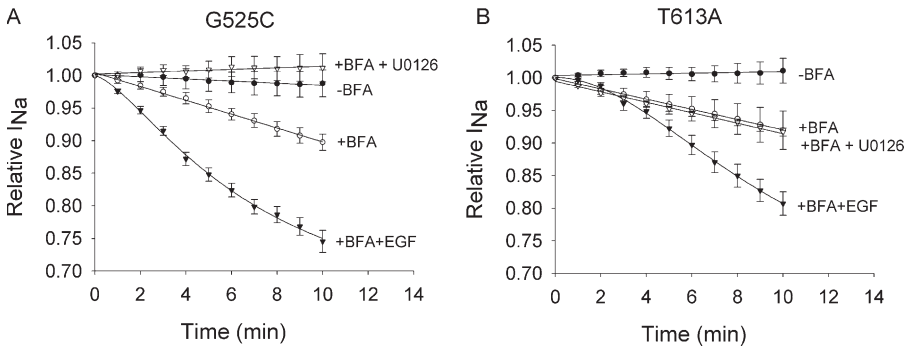

Figure 12. Effect of ERK1/2 phosphorylation on I_{Na} following treatment with brefeldin A. (A and B) G525C and T613A MDCK cells grown to confluence were mounted in Ussing chambers, treated with benzamil (1 μM) to block channels with endogenous β-ENaC subunits and then exposed to vehicle or brefeldin A (20 μM; 30 min, bilateral) to inhibit delivery of new channels to the plasma membrane. At $t = -5$min, monolayers were treated with EGF (20 ng/ml, basolateral) or U0126 (10 μM, bilateral), and 30 min later amiloride (10 mM, apical) was applied. The relative I_{Na} was calculated at 1-min intervals as the I_{Na} at each time point relative to the I_{Na} at $t = 0$. $n = 5$ for each group.

EGF-induced inhibition of ENaC activity did not require ERK activation (Tong and Stockand, 2005).

Point Mutation of the PY Motif and the Putative ERK Phosphorylation Site in β-ENaC

Deletion of the intracellular β-ENaC C terminus eliminates several consensus phosphorylation sites as well as two internalization motifs (PY and YXXφ) important for Nedd4- and dynamin/clathrin-dependent endocytosis. To test the importance of individual sites, point mutations were evaluated. Disruption of the PY motif by mutation of β-ENaC P616L (a human Liddle's disease causing mutation) was as effective as the R564st β-ENaC truncation mutation for preventing the EGF-induced inhibition of sodium absorption in MDCK cell monolayers (Fig. 6). A similar result was obtained from studies of oocytes in which point mutations in the PY motif of either β- or γ-ENaC (Y618A or Y628A, respectively) were found to completely prevent progesterone-induced inhibition of sodium current (Michlig et al., 2005). Whereas, mutation of the putative ERK phosphorylation sites in either β-ENaC (T613A) or γ-ENaC (T623A) reduced the progesterone-induced inhibition of sodium current by only 20–25% (Michlig et al., 2005). In contrast, mutation of the putative ERK phosphorylation site in β-ENaC stably expressed in MDCK cells (T613A) was as effective as the R564st β-ENaC truncation (Fig. 6). Furthermore, the small inhibitory effect of EGF on sodium transport in MDCK cells expressing the R564st, P616L, and T613A mutations was completely abolished by an ERK kinase inhibitor (Fig. 7), consistent with a role for the corresponding PY motif and putative ERK phosphorylation site in the C terminus of the γ-ENaC subunit.

Mechanism of ERK-dependent Inhibition of Sodium Absorption

We have shown previously that the acute, EGF-induced inhibition of amiloride-sensitive I_{sc} in renal epithelial cells is localized to the apical membrane, presumably due to changes in ENaC expression or gating (Falin et al., 2005). EGF receptor-mediated activation of intracellular signaling cascades could lead to changes in membrane potential and/or intracellular ion composition sufficient to alter the electrochemical potential difference for sodium across the apical membrane, but it is difficult to reconcile such a mechanism with the observation that β-ENaC mutations abrogate the ERK-dependent inhibition of sodium absorption. The acute inhibitory effect of EGF on ENaC-mediated sodium absorption could be due to (a) reduced channel delivery to the apical membrane, (b) relative increase in delivery of uncleaved, inactive channels to the apical membrane, (c) enhanced retrieval of active channels from the membrane, or (d) decreased channel open probability.

Channel Delivery

The effects of decreased (U0126) and increased (EGF) ERK1/2 phosphorylation on I_{sc} in BFA-treated monolayers are inconsistent with a major effect of p-ERK1/2 on ENaC delivery (Fig. 12 and Table I). If EGF-induced inhibition of sodium current was due to reduced delivery, then EGF should be ineffective in BFA-treated G525C monolayers. Interestingly, reduction in basal p-ERK1/2 with the ERK kinase inhibitor slowed the decline in I_{sc} in G525C monolayers but had no effect in cells in which the putative ERK phosphorylation site in β-ENaC was mutated (T613A). Similar experiments conducted in the absence of BFA revealed that U0126 increased I_{sc} in G525C monolayers (17.6 ± 4.8%; $n = 5$) but had no effect in T613A monolayers (−0.3 ± 0.6%; $n = 5$), consistent with tonic ERK-mediated regulation of ENaC and sodium absorption.

Channel Cleavage

Recent studies have pointed to the importance of proteolytic cleavage of the α and γ subunits in the activation of ENaC (Hughey et al., 2004; Kleyman et al., 2006; Sheng et al., 2006). Intracellular, membrane anchored,

and soluble proteases have been implicated in ENaC activation (Vuagniaux et al., 2000; Kleyman et al., 2006; Bruns et al., 2007). Excessive sodium absorption seen with Liddle's mutations was found to be due not only to an increase in the number of channels at the plasma membrane (Schild et al., 1995; Snyder et al., 1995), but also in an increase in single channel activity (Firsov et al., 1996). Recently, it was reported that Liddle's mutations (R566X β-ENaC and K576X γ-ENaC) increase the fraction of cleaved, active channels at the plasma membrane of transiently transfected Fisher rat thyroid and HEK 293 cells by 2–50-fold (Knight et al., 2006). Delivery of a greater proportion of uncleaved, inactive channels or a reduced rate of activation of channels at the apical membrane in response to EGF could account for the ERK-dependent decrease in amiloride-sensitive I_{sc}. The results of the BFA (Fig. 12 and Table I) and the exogenous trypsin (Fig. 10) experiments suggest that alterations in channel cleavage cannot explain the EGF-induced inhibition of sodium absorption. Furthermore, we found that exogenous trypsin increased amiloride-sensitive I_{sc} by only a small amount (∼15%) in MDCK cell monolayers expressing wild-type ENaC, a result incompatible with the existence of a large pool of silent, inactive sodium channels in the apical membrane of these cells.

Channel Retrieval

Liddle's syndrome is caused by mutations in ENaC that disrupt or eliminate the PY motifs found in the intracellular C termini of the β and γ subunits, thereby interfering with Nedd4 binding and promoting channel retention in the plasma membrane (Schild et al., 1996; Staub et al., 1996). Garty and coworkers reported ERK-dependent phosphorylation of amino acids near PY motifs in β- and γ-ENaC subunit, namely βT613 and γT623 and enhanced binding to Nedd4 (Shi et al., 2002a). We showed that EGF-induced inhibition of sodium absorption is significantly attenuated by deletion or mutation of the PY motif and mutation of the putative ERK phosphorylation site (Figs. 1 and 6). These results point to enhanced channel retrieval as the mechanism for ERK-mediated inhibition of ENaC activity. A relatively small fraction of ENaC is present at the plasma membrane so it was necessary to evaluate changes in surface expression by apical membrane biotinylation followed by immunoprecipitation of FLAG-tagged β-ENaC. Unexpectedly, we found that surface expression of ENaC was not decreased 30 min after EGF treatment, a time at which EGF-induced inhibition of I_{sc} was fully developed (Figs. 8 and 2). We cannot rule out the possibility that the individual ENaC subunits are differentially retrieved (Mohan et al., 2004). A large pool of inactive channels in the plasma membrane could also mask selective retrieval of a small subpopulation of functional channels. As described in the preceding section, it is unlikely that under the conditions of our experiments, there exist a significant number of inactive channels in the apical membrane. Thus, the failure to detect a decrease in surface expression of ENaC after 30 min exposure to EGF despite the ∼30% decrease in I_{sc} cannot be explained by a large pool of silent channels that obscures selective retrieval of a small number of active channels. Furthermore, we did observe a time-dependent decrease in ENaC surface expression at later time points (60, 90, and 120 min). Despite the fact that EGF-induced inhibition of sodium absorption is sensitive to mutations at sites associated with channel retrieval, our results demonstrate that inhibition occurs without concurrent channel internalization.

Channel Open Probability (P_o)

Since the ∼30% decrease in current elicited by EGF treatment occurs with no change in the apical surface expression of ENaC, the most likely mechanism for the fall in ENaC activity is a reduction in P_o. Michlig et al. (2005) arrived at a similar conclusion based on studies of progesterone-induced inhibition of sodium current in oocytes expressing ENaC subunits. The rapid reversibility of EGF-induced inhibition of I_{sc} at early time points (<30 min; Fig. 11) is also consistent with reversible alterations in channel gating rather than channel retrieval and degradation (Booth and Stockand, 2003). A recent study of wild-type and Liddle's mutants expressed in MDCK cells found poor channel recycling of internalized ENaC (Chen et al., 2007). Introduction of the β-S518K mutation (gating mutant with $P_o \sim 1.0$) did not prevent the early inhibition by EGF, indicating that the mechanism by which EGF inhibits ENaC is independent of the normal gating process that is altered by the S518K modification. In fact, the S518K mutant was inhibited to a greater degree than wild-type ENaC. If EGF-induced inhibition of ENaC function is due to protein modification of ENaC (e.g., subunit ubiquitination) resulting in channel inactivation, then an increase in fractional inhibition would be predicted with the β-S518K mutation. ERK2 can phosphorylate C-terminal peptides from β- and γ-ENaC subunits (Shi et al., 2002a), and progesterone-stimulated phosphorylation of β-ENaC is reduced by mutation of the putative ERK phosphorylation site in β-ENaC (T613A) (Michlig et al., 2005). It is unlikely that phosphorylation of ENaC per se is responsible for the ERK-dependent reduction in ENaC activity since mutation of the adjacent PY motif (Y618A [Michlig et al., 2005] and P616L [Fig. 6]) blocked progesterone and EGF-induced inhibition of sodium current. Additionally, it is improbable that the interaction of Nedd4-2 with ENaC alone results in a decrease with the P_o of ENaC, since expression of a catalytically inactive mutant of Nedd4-2 (Michlig et al., 2005) prevented the progesterone-induced decrease in ENaC activity, though presumably it should be capable of binding the channel.

Ubiquitination of the channel is a possible route by which open probability may be altered. The attachment of the first ubiquitin molecule involves the formation of a bond between ubiquitin's C-terminal glycine and a lysine residue on the target protein. Additional ubiquitin molecules can then be attached to the first through attachment to one of three of its lysine residues: K29, K48, and K63 (Arnason and Ellison, 1994). A polyubiquitin chain consisting of four or more ubiquitin molecules attached through K48 is a characteristic signal targeting proteins for degradation in the 26S proteasome (Thrower et al., 2000). Recently a ubiquitin-specific protease, Usp2-45, was identified among the early gene products expressed in response to aldosterone in the mouse distal nephron. This protein can deubiquitinate ENaC, resulting in an increase in sodium absorption (Fakitsas et al., 2007). The identification of new classes of ubiquitin binding proteins and deubiquitinating enzymes thought to be involved in the processing and regulation of internalization (Hicke and Dunn, 2003; Clague and Urbe, 2006) add an additional level of complexity to the regulation of ubiquitination.

Michlig et al. (2005) found from their studies of ENaC expressed in oocytes that progesterone caused an ~80% reduction in sodium current with no significant change in ENaC surface expression and concluded that the primary effect was a decrease in channel P_o (although P_o was not directly measured). In contrast, we found that EGF caused a smaller reduction in sodium current (~30%) and after a delay of >30 min, surface expression of ENaC was reduced. This is consistent with an early decrease in channel P_o (conclusion based on no detectable decrement in surface expression within 30 min after EGF treatment), though we have not measured P_o directly. There are several possible explanations for why the secondary decrease in surface expression was observed in MDCK cells but not in oocytes. First, the mechanisms may be fundamentally different in oocytes and mammalian epithelial cells. Second, a significant portion of the progesterone-induced decrease in sodium current may be ERK independent. EGF-simulated ERK1/2 phosphorylation and inhibition of sodium absorption in mouse collecting duct cells and MDCK cells was rapid (5–15 min) and completely blocked by treatment with an ERK kinase inhibitor. While progesterone has been shown to increase ERK phosphorylation at 6 and 12 h in oocytes (Nicod et al., 2002; Soundararajan et al., 2005), the progesterone-induced decrease in sodium current is nearly maximal at 30 min, and Frisov and coworkers did not show that progesterone-induced inhibition of sodium current was prevented by an ERK kinase inhibitor (Nicod et al., 2002; Michlig et al., 2005). Third, ENaC expression in oocytes results in delivery of a significant fraction (90%) (Vallet et al., 2002) of inactive channels to the plasma membrane (i.e., channels that can be activated by extracellular trypsin), thus a correlation between changes in amiloride-sensitive current and biochemical estimates of surface expression may be tenuous.

In summary, our results are consistent with an ERK-mediated decrease in channel P_o and enhanced removal of ENaC from the apical membrane. The importance of the examination of ERK-mediated control of sodium absorption is twofold. First, in autosomal recessive polycystic kidney disease, mislocalization of the EGF receptor to the apical membrane results in chronic activation of ERK1/2 (Veizis and Cotton, 2005). The resulting inhibition in sodium absorption is believed to contribute to disease progression (Omori et al., 2006). Second, although this study deals with the EGF-induced inhibition in ENaC activity, other agonists, including extracellular ATP and PMA (Falin et al., 2005), inhibit sodium absorption partially via an ERK-mediated mechanism and these results may aid in our understanding of those processes.

The authors wish to thank Drs. Hummler and Rossier for providing the transgenic Liddle's mice for these studies. We also thank Mike Haley, Elizabeth Carroll, and Mike Wilson for expert technical assistance and Elias Veizis for helpful discussions.

This study was supported by Polycystic Kidney Disease Foundation, American Heart Association, and National Institute of Diabetes and Digestive and Kidney Diseases grants P50-DK57306 and P30-DK27651. Rebecca Falin was supported by National Institutes of Health grant T32-DK007678.

Lawrence G. Palmer served as editor.

Submitted: 2 March 2007
Accepted: 10 August 2007

REFERENCES

Arnason, T., and M.J. Ellison. 1994. Stress resistance in *Saccharomyces cerevisiae* is strongly correlated with assembly of a novel type of multiubiquitin chain. *Mol. Cell. Biol.* 14:7876–7883.

Auberson, M., N. Hoffmann-Pochon, A. Vandewalle, S. Kellenberger, and L. Schild. 2003. Epithelial Na^+ channel mutants causing Liddle's syndrome retain ability to respond to aldosterone and vasopressin. *Am. J. Physiol. Renal Physiol.* 285:F459–F471.

Blazer-Yost, B.L., X. Liu, and S.I. Helman. 1998. Hormonal regulation of ENaCs: insulin and aldosterone. *Am. J. Physiol.* 274: C1373–C1379.

Booth, R.E., and J.D. Stockand. 2003. Targeted degradation of ENaC in response to PKC activation of the ERK1/2 cascade. *Am. J. Physiol. Renal Physiol.* 284:F938–F947.

Bruns, J.B., M.D. Carattino, S. Sheng, A.B. Maarouf, O.A. Weisz, J.M. Pilewski, R.P. Hughey, T.R. Kleyman. 2007. Epithelial Na^+ channels are fully activated by furin- and prostasin-dependent release of an inhibitory peptide from the γ subunit. *J. Biol. Chem.* 282:6153–6160.

Cano, E., and L.C. Mahadevan. 1995. Parallel signal processing among mammalian MAPKs. *Trends Biochem. Sci.* 20:117–122.

Chen, H.I., and M. Sudol. 1995. The WW domain of Yes-associated protein binds a proline-rich ligand that differs from the consensus established for Src homology 3-binding modules. *Proc. Natl. Acad. Sci. USA.* 92:7819–7823.

Chen, L., S. Pribanic, A. Debonneville, C. Jiang, and D. Rotin. 2007. The PY-motif of ENaC, mutated in Liddle syndrome, regulates channel internalization, sorting and mobilization from sub-apical pool. *Traffic.* 8:1246–1264.

Chigaev, A., G. Lu, H. Shi, C. Asher, R. Xu, H. Latter, R. Seger, H. Garty, and E. Reuveny. 2001. In vitro phosphorylation of COOH termini of the epithelial Na^+ channel and its effects on channel activity in *Xenopus* oocytes. *Am. J. Physiol. Renal Physiol.* 280: F1030–F1036.

Clague, M.J., and S. Urbe. 2006. Endocytosis: the DUB version. *Trends Cell Biol.* 16:551–559.

Cobb, M.H. 1999. MAP kinase pathways. *Prog. Biophys. Mol. Biol.* 71:479–500.

Condliffe, S.B., H. Zhang, and R.A. Frizzell. 2004. Syntaxin 1A regulates ENaC channel activity. *J. Biol. Chem.* 279:10085–10092.

Dahlmann, A., S. Pradervand, E. Hummler, B.C. Rossier, G. Frindt, and L.G. Palmer. 2003. Mineralocorticoid regulation of epithelial Na^+ channels is maintained in a mouse model of Liddle's syndrome. *Am. J. Physiol. Renal Physiol.* 285:F310–F318.

Danto, S.I., Z. Borok, X.L. Zhang, M.Z. Lopez, P. Patel, E.D. Crandall, and R.L. Lubman. 1998. Mechanisms of EGF-induced stimulation of sodium reabsorption by alveolar epithelial cells. *Am. J. Physiol.* 275:C82–C92.

Fakitsas, P., G. Adam, D. Daidie, M.X. van Bemmelen, F. Fouladkou, A. Patrignani, U. Wagner, R. Warth, S.M. Camargo, O. Staub, and F. Verrey. 2007. Early aldosterone-induced gene product regulates the epithelial sodium channel by deubiquitylation. *J. Am. Soc. Nephrol.* 18:1084–1092.

Falin, R., I.E. Veizis, and C.U. Cotton. 2005. A role for ERK1/2 in EGF- and ATP-dependent regulation of amiloride-sensitive sodium absorption. *Am. J. Physiol. Cell Physiol.* 288:C1003–C1011.

Firsov, D., L. Schild, I. Gautschi, A.M. Merillat, E. Schneeberger, and B.C. Rossier. 1996. Cell surface expression of the epithelial Na channel and a mutant causing Liddle syndrome: a quantitative approach. *Proc. Natl. Acad. Sci. USA.* 93:15370–15375.

Garty, H., and L.G. Palmer. 1997. Epithelial sodium channels: function, structure, and regulation. *Physiol. Rev.* 77:359–396.

Hicke, L., and R. Dunn. 2003. Regulation of membrane protein transport by ubiquitin and ubiquitin-binding proteins. *Annu. Rev. Cell Dev. Biol.* 19:141–172.

Hughey, R.P., G.M. Mueller, J.B. Bruns, C.L. Kinlough, P.A. Poland, K.L. Harkleroad, M.D. Carattino, and T.R. Kleyman. 2003. Maturation of the epithelial Na^+ channel involves proteolytic processing of the α- and γ-subunits. *J. Biol. Chem.* 278:37073–37082.

Hughey, R.P., J.B. Bruns, C.L. Kinlough, K.L. Harkleroad, Q. Tong, M.D. Carattino, J.P. Johnson, J.D. Stockand, and T.R. Kleyman. 2004. Epithelial sodium channels are activated by furin-dependent proteolysis. *J. Biol. Chem.* 279:18111–18114.

Hummler, E. 2003. Epithelial sodium channel, salt intake, and hypertension. *Curr. Hypertens. Rep.* 5:11–18.

Kari, C., T.O. Chan, M. Rocha de Quadros, and U. Rodeck. 2003. Targeting the epidermal growth factor receptor in cancer: apoptosis takes center stage. *Cancer Res.* 63:1–5.

Kleyman, T.R., M.M. Myerburg, and R.P. Hughey. 2006. Regulation of ENaCs by proteases: an increasingly complex story. *Kidney Int.* 70:1391–1392.

Knight, K.K., D.R. Olson, R. Zhou, and P.M. Snyder. 2006. Liddle's syndrome mutations increase Na^+ transport through dual effects on epithelial Na^+ channel surface expression and proteolytic cleavage. *Proc. Natl. Acad. Sci. USA.* 103:2805–2808.

Lingueglia, E., N. Voilley, R. Waldmann, M. Lazdunski, and P. Barbry. 1993. Expression cloning of an epithelial amiloride-sensitive Na^+ channel. A new channel type with homologies to *Caenorhabditis elegans* degenerins. *FEBS Lett.* 318:95–99.

Michlig, S., M. Harris, J. Loffing, B.C. Rossier, and D. Firsov. 2005. Progesterone down-regulates the open probability of the amiloride-sensitive epithelial sodium channel via a Nedd4-2-dependent mechanism. *J. Biol. Chem.* 280:38264–38270.

Mohan, S., J.R. Bruns, K.M. Weixel, R.S. Edinger, J.B. Bruns, T.R. Kleyman, J.P. Johnson, and O.A. Weisz. 2004. Differential current decay profiles of epithelial sodium channel subunit combinations in polarized renal epithelial cells. *J. Biol. Chem.* 279:32071–32078.

Morris, R.G., and J.A. Schafer. 2002. cAMP increases density of ENaC subunits in the apical membrane of MDCK cells in direct proportion to amiloride-sensitive Na^+ transport. *J. Gen. Physiol.* 120:71–85.

Nicod, M., S. Michlig, M. Flahaut, M. Salinas, N. Fowler Jaeger, J.D. Horisberger, B.C. Rossier, and D. Firsov. 2002. A novel vasopressin-induced transcript promotes MAP kinase activation and ENaC downregulation. *EMBO J.* 21:5109–5117.

Omori, S., M. Hida, H. Fujita, H. Takahashi, S. Tanimura, M. Kohno, and M. Awazu. 2006. Extracellular signal-regulated kinase inhibition slows disease progression in mice with polycystic kidney disease. *J. Am. Soc. Nephrol.* 17:1604–1614.

Pearson, G., F. Robinson, T. Beers Gibson, B.E. Xu, M. Karandikar, K. Berman, and M.H. Cobb. 2001. Mitogen-activated protein (MAP) kinase pathways: regulation and physiological functions. *Endocr. Rev.* 22:153–183.

Pradervand, S., A. Vandewalle, M. Bens, I. Gautschi, J. Loffing, E. Hummler, L. Schild, and B.C. Rossier. 2003. Dysfunction of the epithelial sodium channel expressed in the kidney of a mouse model for Liddle syndrome. *J. Am. Soc. Nephrol.* 14:2219–2228.

Pradervand, S., Q. Wang, M. Burnier, F. Beermann, J.D. Horisberger, E. Hummler, and B.C. Rossier. 1999. A mouse model for Liddle's syndrome. *J. Am. Soc. Nephrol.* 10:2527–2533.

Renard, S., E. Lingueglia, N. Voilley, M. Lazdunski, and P. Barbry. 1994. Biochemical analysis of the membrane topology of the amiloride-sensitive Na+ channel. *J. Biol. Chem.* 269:12981–12986.

Rossier, B.C. 2002. Hormonal regulation of the epithelial sodium channel ENaC: N or P(o)? *J. Gen. Physiol.* 120:67–70.

Rossier, B.C., S. Pradervand, L. Schild, and E. Hummler. 2002. Epithelial sodium channel and the control of sodium balance: interaction between genetic and environmental factors. *Annu. Rev. Physiol.* 64:877–897.

Rotin, D., D. Bar-Sagi, H. O'Brodovich, J. Merilainen, V.P. Lehto, C.M. Canessa, B.C. Rossier, and G.P. Downey. 1994. An SH3 binding region in the epithelial Na^+ channel (α rENaC) mediates its localization at the apical membrane. *EMBO J.* 13:4440–4450.

Schafer, J.A. 2002. Abnormal regulation of ENaC: syndromes of salt retention and salt wasting by the collecting duct. *Am. J. Physiol. Renal Physiol.* 283:F221–F235.

Schild, L., M. Canessa, R.A. Shimkets, I. Gautschi, R.P. Lifton, and B.C. Rossier. 1995. A mutation in the epithelial sodium channel causing Liddle disease increases channel activity in the *Xenopus laevis* oocyte expression system. *Proc. Natl. Acad. Sci. USA.* 92:5699–5703.

Schild, L., Y. Lu, I. Gautschi, E. Schneeberger, R.P. Lifton, and B.C. Rossier. 1996. Identification of a PY motif in the epithelial Na channel subunits as a target sequence for mutations causing channel activation found in Liddle syndrome. *EMBO J.* 15:2381–2387.

Schild, L., E. Schneeberger, I. Gautschi, and D. Firsov. 1997. Identification of amino acid residues in the α, β, and γ subunits of the epithelial sodium channel (ENaC) involved in amiloride block and ion permeation. *J. Gen. Physiol.* 109:15–26.

Shen, J.P., and C.U. Cotton. 2003. Epidermal growth factor inhibits amiloride-sensitive sodium absorption in renal collecting duct cells. *Am. J. Physiol. Renal Physiol.* 284:F57–F64.

Sheng, S., M.D. Carattino, J.B. Bruns, R.P. Hughey, T.R. Kleyman. 2006. Furin cleavage activates the epithelial Na^+ channels by relieving Na^+ self-inhibition. *Am. J. Physiol. Renal. Physiol.* 290: F1488–F1496.

Shi, H., C. Asher, A. Chigaev, Y. Yung, E. Reuveny, R. Seger, and H. Garty. 2002a. Interactions of β and γ ENaC with Nedd4 can be facilitated by an ERK-mediated phosphorylation. *J. Biol. Chem.* 277:13539–13547.

Shi, H., C. Asher, Y. Yung, L. Kligman, E. Reuveny, R. Seger, and H. Garty. 2002b. Casein kinase 2 specifically binds to and phosphorylates the carboxy termini of ENaC subunits. *Eur. J. Biochem.* 269:4551–4558.

Snyder, P.M., C. Cheng, L.S. Prince, J.C. Rogers, and M.J. Welsh. 1998. Electrophysiological and biochemical evidence that DEG/ENaC cation channels are composed of nine subunits. *J. Biol. Chem.* 273:681–684.

Snyder, P.M.F.J. McDonaldJ.B. StokesM.J. Welsh. 1994. Membrane topology of the amiloride-sensitive epithelial sodium channel. *J. Biol. Chem.* 269:24379–24383.

Snyder, P.M., M.P. Price, F.J. McDonald, C.M. Adams, K.A. Volk, B.G. Zeiher, J.B. Stokes, and M.J. Welsh. 1995. Mechanism by which Liddle's syndrome mutations increase activity of a human epithelial Na^+ channel. *Cell.* 83:969–978.

Soundararajan, R., T.T. Zhang, J. Wang, A. Vandewalle, and D. Pearce. 2005. A novel role for glucocorticoid-induced leucine zipper protein in epithelial sodium channel-mediated sodium transport. *J. Biol. Chem.* 280:39970–39981.

Srinivas, S., M.R. Goldberg, T. Watanabe, V. D'Agati, Q. al-Awqati, and F. Costantini. 1999. Expression of green fluorescent protein in the ureteric bud of transgenic mice: a new tool for the analysis of ureteric bud morphogenesis. *Dev. Genet.* 24:241–251.

Staruschenko, A., E. Adams, R.E. Booth, and J.D. Stockand. 2005. Epithelial Na^+ channel subunit stoichiometry. *Biophys. J.* 88:3966–3975.

Staub, O., H. Abriel, P. Plant, T. Ishikawa, V. Kanelis, R. Saleki, J.D. Horisberger, L. Schild, and D. Rotin. 2000. Regulation of the epithelial Na^+ channel by Nedd4 and ubiquitination. *Kidney Int.* 57:809–815.

Staub, O., S. Dho, P. Henry, J. Correa, T. Ishikawa, J. McGlade, and D. Rotin. 1996. WW domains of Nedd4 bind to the proline-rich PY motifs in the epithelial Na^+ channel deleted in Liddle's syndrome. *EMBO J.* 15:2371–2380.

Staub, O., I. Gautschi, T. Ishikawa, K. Breitschopf, A. Ciechanover, L. Schild, and D. Rotin. 1997. Regulation of stability and function of the epithelial Na^+ channel (ENaC) by ubiquitination. *EMBO J.* 16:6325–6336.

Stutts, M.J., C.M. Canessa, J.C. Olsen, M. Hamrick, J.A. Cohn, B.C. Rossier, and R.C. Boucher. 1995. CFTR as a cAMP-dependent regulator of sodium channels. *Science.* 269:847–850.

Thrower, J.S., L. Hoffman, M. Rechsteiner, and C.M. Pickart. 2000. Recognition of the polyubiquitin proteolytic signal. *EMBO J.* 19:94–102.

Tong, Q., and J.D. Stockand. 2005. Receptor tyrosine kinases mediate epithelial Na^+ channel inhibition by epidermal growth factor. *Am. J. Physiol. Renal Physiol.* 288:F150–F161.

Vallet, V., C. Pfister, J. Loffing, and B.C. Rossier. 2002. Cell-surface expression of the channel activating protease xCAP-1 is required for activation of ENaC in the *Xenopus* oocyte. *J. Am. Soc. Nephrol.* 13:588–594.

Veizis, E.I., C.R. Carlin, and C.U. Cotton. 2004. Decreased amiloride-sensitive Na^+ absorption in collecting duct principal cells isolated from BPK ARPKD mice. *Am. J. Physiol. Renal Physiol.* 286:F244–F254.

Veizis, I.E., and C.U. Cotton. 2005. Abnormal EGF-dependent regulation of sodium absorption in ARPKD collecting duct cells. *Am. J. Physiol. Renal Physiol.* 288:F474–F482.

Voilley, N., A. Galibert, F. Bassilana, S. Renard, E. Lingueglia, S. Coscoy, G. Champigny, P. Hofman, M. Lazdunski, and P. Barbry. 1997. The amiloride-sensitive Na^+ channel: from primary structure to function. *Comp. Biochem. Physiol. A Physiol.* 118:193–200.

Voilley, N., E. Lingueglia, G. Champigny, M.G. Mattei, R. Waldmann, M. Lazdunski, and P. Barbry. 1994. The lung amiloride-sensitive Na^+ channel: biophysical properties, pharmacology, ontogenesis, and molecular cloning. *Proc. Natl. Acad. Sci. USA.* 91:247–251.

Vuagniaux, G., V. Vallet, N.F. Jaeger, C. Pfister, M. Bens, N. Farman, N. Courtois-Coutry, A. Vandewalle, B.C. Rossier, and E. Hummler. 2000. Activation of the amiloride-sensitive epithelial sodium channel by the serine protease mCAP1 expressed in a mouse cortical collecting duct cell line. *J. Am. Soc. Nephrol.* 11:828–834.

Warnock, D.G. 2001. Liddle syndrome: genetics and mechanisms of Na^+ channel defects. *Am. J. Med. Sci.* 322:302–307.

Yang, L.M., R. Rinke, C. Korbmacher. 2006. Stimulation of the epithelial sodium channel (ENaC) by cAMP involves putative ERK phosphorylation sites in the C termini of the channel's β- and γ-subunit. *J. Biol. Chem.* 281:9859–9868.

Zhang, Y.H., D. Alvarez de la Rosa, C.M. Canessa, and J.P. Hayslett. 2005. Insulin-induced phosphorylation of ENaC correlates with increased sodium channel function in A6 cells. *Am. J. Physiol. Cell Physiol.* 288:C141–C147.